Neuron, Vol. 35, 1147–1156, September 12, 2002, Copyright ©2002 by Cell Press

# Human Brain Activity during Illusory Visual Jitter as Revealed by Functional Magnetic Resonance Imaging

**Yuka Sasaki,[1,4] Ikuya Murakami,[2] Patrick Cavanagh,[3] and Roger H.B. Tootell[1]**
[1]Athinoula A. Martinos Center for Biomedical Imaging
Massachusetts General Hospital
149 13th Street
Charlestown, Massachusetts 02129
[2]Human and Information Science Laboratory
NTT Communication Science Laboratories
NTT Corporation
3-1 Morinosato Wakamiya
Atsugi, Kanagawa 243-0198
Japan
[3]Vision Sciences Laboratory
Department of Psychology
Harvard University
33 Kirkland Street
Cambridge, Massachusetts 02138

## Summary

**One central problem in vision is how to compensate for retinal slip. A novel illusion (visual jitter) suggests the compensation mechanism is based solely on retinal motion. Adaptation to visual noise attenuates the motion signals used by the compensation stage, producing illusory jitter due to the undercompensation of retinal slip. Here, we investigated the neural substrate of retinal slip compensation during this illusion using high-field fMRI and retinotopic mapping in flattened cortical format. When jitter perception occurred, MR signal decreased in lower stages of the visual system but increased prominently in area MT+. In conclusion, visual areas as early as V1 are responsible for the adaptation stage, and MT+ is involved in the compensation stage. The present finding suggests the pathway from V1 to MT+ has an important role in stabilizing the visual world.**

## Introduction

Whenever the eyes move, there is concomitant retinal image slip of a stationary outer world at a speed corresponding to the rotation speed of the eyes. Importantly, such a retinal slip is usually not noticed. Clearly, the brain somehow compensates for retinal slip due to eye movements in recovering a veridical visual world. However, under certain circumstances we can defeat the compensation and perceive our own retinal slip. Specifically, after adaptation to a patch (e.g., an annulus) of dynamic random noise, a larger pattern of static random noise is presented. The static noise in the unadapted region then appears to "jitter" coherently in random directions for several seconds (please access the visual jitter demonstration [first figure] at http://www.brl.ntt.co.jp/people/ikuya/). This jittery motion has been demonstrated to reflect retinal slip due to small eye movements that are normally kept invisible (Murakami and Cavanagh, 1998).

This unique illusion suggests a specific way that the brain may normally cancel the motion signals from small eye movements. Murakami and Cavanagh (1998, 2001) have proposed that retinal motion signals can be used to compensate for retinal slip due to small eye movements. They postulate two stages of the process. The first is an adaptable stage that measures local motion signals, and the second is a compensation stage that estimates retinal slip and subtracts it from motion signals nearby.

Suppose that retinal slip is fully represented in early visual cortex (Galletti et al., 1984; Gur et al., 1997; Gur and Snodderly, 1987, 1997; Ilg and Thier, 1996; Leopold and Logothetis, 1998). In this early stage, each retinotopic point is assumed to have a motion vector (direction and speed) that is a mixture of eye movements and object motion. One of the missions of a subsequent processing stage is to suppress the component of eye movements in this velocity field. It is proposed that a baseline value (i.e., eye velocity) is estimated by finding the region having the minimum instantaneous velocity. The minimum velocity will usually arise in regions of the scene where there is no external motion and, so, will represent the eye movement velocity alone. By subtracting this baseline estimate from the velocities of all points, the desired zero velocity for the stationary regions and the correct velocity for the moving objects could be recovered.

This model also explains why the visual jitter illusion occurs. First, adaptation to dynamic noise desensitizes motion detectors in the adapted region. This means that the retinal slip after adaptation is encoded with a smaller gain in the adapted region, although there is no change in small eye movements and corresponding retinal slip with and without adaptation. This creates a new baseline minimum there. In the unadapted region, the unattenuated motion response to eye movements is above this new, artificially low baseline. Therefore, the retinal slip occurring in this region is undercompensated and is perceived as jitter.

Visual jitter clearly differs from the classical motion aftereffect (an illusory motion in the opposite direction after adaptation to unidirectional motion [Wohlgemuth, 1911]). First, jitter occurs in the unadapted region, while conventional motion aftereffect is confined within the adapted region (Culham et al., 1999; He et al., 1998). Second, the instantaneous speed and direction of jitter are consistent with eye movements during test, whereas the direction of motion aftereffect is opposite to the direction of the adapting stimulus. Third, motion aftereffect partially transfers across eyes (Ibbotson and Maddess, 1994; Murakami, 1995; Wade et al., 1993), but visual jitter does not (Murakami and Cavanagh, 1998). Therefore, these two types of illusions are distinct from each other.

As described before, the proposed mechanism of the jitter aftereffect postulates two distinct stages: (1) an early adaptable stage where local motion signals are

[4]Correspondence: yuka@nmr.mgh.harvard.edu

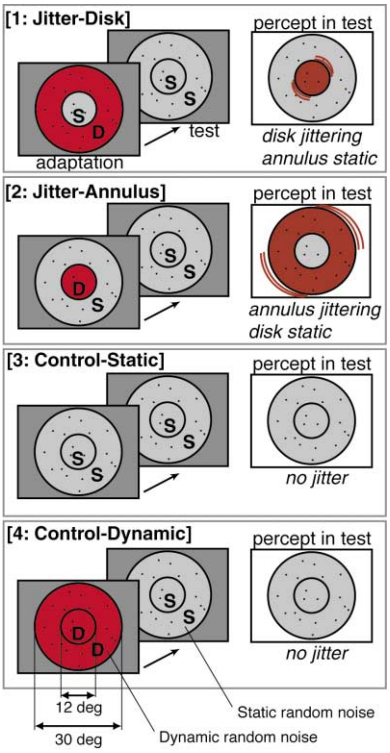


Figure 1. Visual Stimulus Configuration

There were four conditions, with one condition being presented in each box: 1, jitter-disk; 2, jitter-annulus; 3, control-static; and 4, control-dynamic. In each condition, a trial consisted of an adaptation period (32 s) and a subsequent test period (32 s). The adapting stimulus varied across conditions. The letter D indicates dynamic random noise (also emphasized by red in this figure) and the letter S indicates static random noise. In the test period, the visual stimulus was identical throughout the four conditions (i.e., static random noise occupied both regions). However, perception in the test period differed across conditions. For illustrative purposes, noise is shown as if sparse, but actually it was 50% density.

encoded and (2) a compensation stage where visual jitter is represented explicitly. The present study tests for the location of each of these two stages (adaptation and compensation) by using functional magnetic resonance imaging (fMRI). In addition to testing whether or not the above model is correct, it is of interest to identify the areas in the visual system that exhibit the effects of adaptation and jitter. Specifically, we mapped visual cortical activity while subjects were looking at stimuli that generate the visual jitter illusion (e.g., adaptation to dynamic noise and subsequent test in static noise). There were four presentation conditions, as depicted in Figure 1. As a result, two distinct activity patterns emerged at different stages of visual cortical hierarchy: an MR signal decrease after adaptation to dynamic noise was observed in lower areas, whereas higher areas showed an increase when the observer perceived jitter. In conjunction with previous psychophysical findings (Murakami and Cavanagh, 1998), these findings lead to tentative brain localization of the two psychophysical stages.

## Results

FMRI experiments were carried out in a 3T scanner in eight normal subjects, using flattened cortical analysis at a spatial resolution of $3 \times 3 \times 3$ mm. Data were shifted by 4 s to compensate for the known hemodynamic delay.

### Retinotopic Representation of Stimulus Regions

First, we tested if retinotopically separate regions were activated by our concentric stimuli for visual jitter. Note that in jitter-disk and jitter-annulus conditions in Figure 1, jitter perception occurs at different retinotopic regions—although the test stimulus was identical. That is, jitter occurs in the disk after the annulus was adapted, whereas jitter occurs in the annulus after adaptation in the disk. In both cases, jitter is confined within the retinotopically unadapted region. Figure 2A shows the retinotopic representation of eccentricity in the right occipital cortex of one representative subject, with borders between the visual areas superimposed. Figure 2B shows the differential BOLD (blood oxygenation level dependent) activity (p value map) obtained by subtracting the activity in the first 10 s of the test period for the jitter-annulus condition (in which jitter was perceived in the annulus) from the activity in the first 10 s of the test period for the jitter-disk condition (in which jitter was perceived in the disk) within the same flattened cortex. The differential BOLD activities were positive (red-orange) in retinotopically central regions and negative (blue-cyan) in more peripheral regions (see Figure 2B). According to the eccentricity map from the same subject, these two cortical regions corresponded to the representations of the disk and annulus in the visual stimulus.

Thus, two points were clearly revealed. First, in the central representations of V1, V2, and other retinotopic areas, the activity of the disk representation was significantly greater for the jitter-disk condition than for jitter-annulus. Second, the opposite pattern of activation was found in the more peripheral retinotopic representations of the annulus: activities in these regions were significantly greater for the jitter-annulus condition. Since the test stimulus was identical (thus cancelling out in the subtractive analysis), these activation patterns during test should be due to the effects of adaptation.

Does this result reflect the neural correlate of visual jitter, or is it a result of neural adaptation uncorrelated with perception? A critical test is to compare the activity in the test period of the jitter-disk condition with that of the control-static condition. In the jitter-disk condition, the annulus was adapted to dynamic noise and the disk appeared to jitter. In the control-static condition, neither the disk nor the annulus was adapted, and neither appeared to jitter. If the differential activity reflects jitter perception, it should be confined within the disk representation. If, on the other hand, the activity reflects neural adaptation, it should be confined within the annulus representation.

We found that the latter was actually the case: the annulus representation (which had been exposed to dynamic random noise in the adaptation period of the jitter-disk condition) gave rise to a significant signal decrease

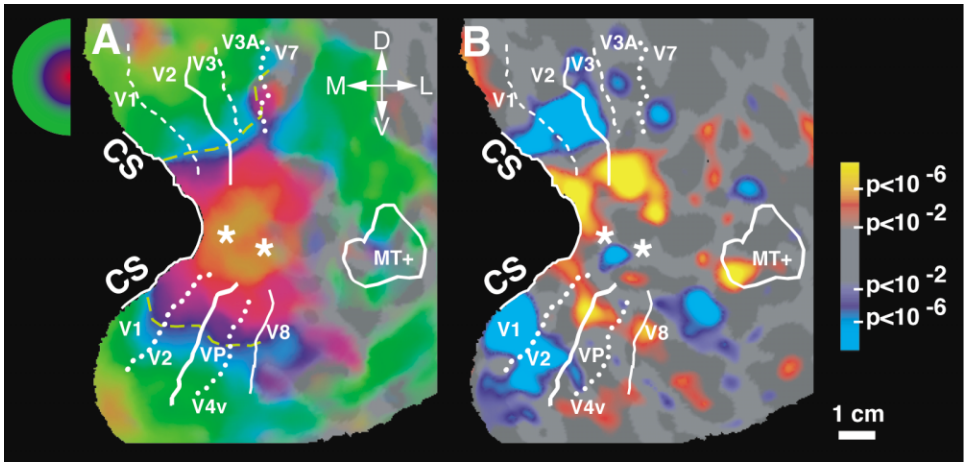


Figure 2. The Visual Cortex in the Right Hemisphere of One Representative Subject Shown in Flattened Format with Borders between Visual Areas

(A) The representation of retinotopic eccentricity, as revealed by phase-encoded mapping. As shown in the legend, red indicates the foveal representation, and progressively more peripheral eccentricities are coded blue, and then green. The retinotopic border between disk and annulus representations in eccentricity are shown as dashed yellow line. The calcarine sulcus is indicated by the letters CS. Asterisks indicate the foveal representations, which are located near the occipital pole.

(B) Differential BOLD activity between conditions jitter-disk and jitter-annulus for the first 10 s of the test period. Blue-cyan regions indicate lower BOLD activity ($p < 0.01$) in jitter-disk than in jitter-annulus conditions, and red-yellow regions indicate higher activity ($p < 0.01$), indicated by the pseudo color scale.

compared to that of the control-static condition (compare [1] and [3] of Figure 3B; see below for details). This signal decrease was observed in V1 and other retinotopic cortical areas. In contrast, there was no comparable change in activation in the disk representation in early visual areas. Thus, the decrease in activity observed in lower visual areas seems to result from neural adaptation at the regions that were exposed to dynamic noise.

In MT+, however, a conspicuous increase in BOLD signals was seen in conditions jitter-disk and jitter-annulus, compared to control-static. Simple neural adaptation cannot explain this increase. Below we conducted more detailed analyses to clarify the sources of this and other activation patterns.

### Region of Interest

In order to reveal the time course of BOLD activity, we defined the region of interest (ROI) in two ways. The first approach was based on retinotopic representations. The representations of the disk and annulus were immediately obvious as iso-eccentric semicircular shapes, and were clearly segregated in V1, V2, V3, VP, V3A, and V4v (see Figure 2). Their border could be confirmed based on the retinotopic eccentricity map from the same subject (cf. Figures 2A and 2B). To analyze the data on this disk versus annulus basis, we defined the group of voxels that reached a significant difference between conditions as the ROI for each of the disk and annulus representations and each visual area. In less retinotopic visual areas such as MT+, we defined the ROI over the entire functionally defined (moving versus stationary) visual area.

The time course data from these ROIs were averaged for each hemisphere and normalized as the percent signal change from their grand mean value. Then they were averaged across hemispheres and subjects.

### Activity Reduction after Adaptation to Dynamic Random Noise

Figures 3A and 3B show the time courses from the retinotopic analysis. The signal changes are plotted as a function of time (with 0 and 32 being the beginning of the adaptation and test periods, respectively). The data from several cortical areas (indicated by colors) are overlaid. The signal changes in the ROI of the disk representation are plotted in Figure 3A. Figure 3B shows the analogous results from the annulus representation. The data for the four conditions (see Figure 1) are plotted in separate panels.

In the control-static condition, no discernible MR change was observed in either the adaptation or test period (Figures 3A and 3B, see [3: control-static]). This is presumably because the visual stimulus was identical throughout the trial. Thus below, all the results in other conditions will be described relative to this stable baseline activity.

What happens after prolonged exposure to dynamic random noise? In the control-dynamic condition, dynamic noise presented in both the disk and annulus regions changed abruptly to static noise after adaptation without producing a jitter aftereffect in either region (Figure 1). As clearly seen, the dynamic noise per se produced an MR signal increase (i.e., greater than the baseline activity in [3]) during the adaptation period (Figures 3A and 3B, see [4: control-dynamic]). Then, however, strong negative activity (i.e., less than the baseline) was observed in both the disk and annulus representations during the subsequent test period. This tendency was most pronounced in V1. Similar responses were

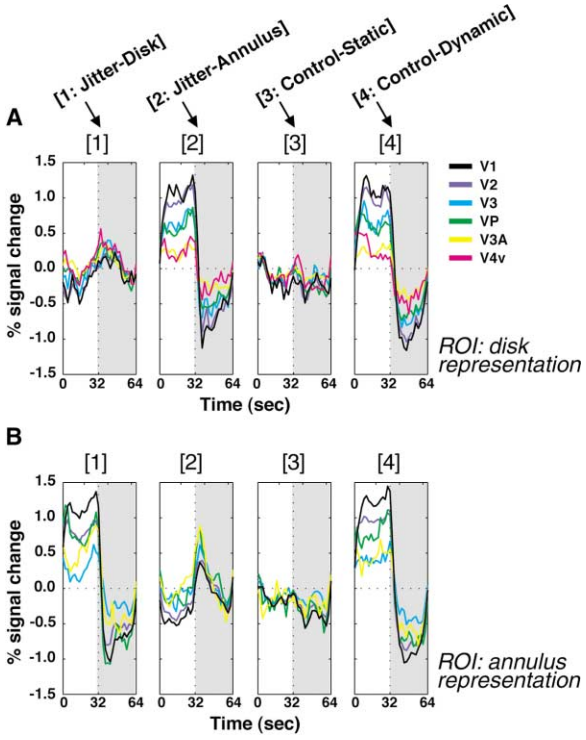


Figure 3. Time Course Results of the Retinotopic Analysis

MR signal changes are plotted in separate panels for the four conditions. (A) shows the latency-corrected time course of the signal change in each visual area (black, V1; purple, V2; cyan, V3; green, VP; yellow, V3A; magenta, V4v) in the disk representation during adaptation (0–32 s) and subsequent test (32–64 s; indicated by gray). (B) shows the same analysis for the annulus representation. No subject showed activation in the annulus representation in V4v. The ordinate indicates the signal change relative to the average activity level across all the conditions; thus its zero level had no functional meaning. Instead, the virtually flat profiles in the control-static condition (3) were considered to reflect the baseline activity relative to which the signal changes were assessed in other conditions.

obtained in higher visual areas, albeit with progressively smaller gains.

Because the test stimulus was identical for all conditions, these MR decreases presumably reflect the effect of adaptation to dynamic random noise. Note that the control-dynamic condition never yielded a visual jitter aftereffect (see Figure 1) after adaptation to dynamic noise. Thus, subsequently observed static noise was as stable as in the adaptation-free visual world. However, the brain activity during the control-dynamic condition was not the same as during the control-static condition. In the control-dynamic condition, there was a negative aftereffect in the MR signals.

What happens in the brain during the test period (in conditions jitter-disk and jitter-annulus) after dynamic random noise was switched to static noise, when jitter was actually perceived? In the jitter-disk condition, MR decreases were observed in the annulus representation during the test period (Figure 3B), whereas the MR signal increased modestly in the disk representation (Figure 3A) during the same period. Similarly, in the jitter-annulus condition, negative MR activity was observed in the disk representation during the test period (Figure 3A), and a relatively steep MR increase was seen in the annulus representation (Figure 3B). In both conditions, the MR signals decreased in the representation of the adapted region after exposure to dynamic random noise, whereas the unadapted region (where jitter was perceived) showed an increase of MR signals. We interpret these MR decreases as reflecting the effect of the dynamic random noise adaptation stimulus. The MR increases are consistent with the occurrence of jitter in these regions.

In the retinotopic analysis, both the MR increases during adaptation and the decreases during the test period were most prominent in V1 and progressively less pronounced as the processing stage increased from V1 to V3 or V4v ([2] and [4] of Figure 3A and [1] and [4] of Figure 3B). In comparison, the positive activity in the test period was more pronounced as the processing stage increased ([1] of Figure 3A and [2] of Figure 3B). Thus, an effect of adaptation was more evident in lower cortical areas, whereas jitter-consistent activity appeared to increase in higher order motion-selective cortical areas.

Subsequent tests confirmed that the MR signal reduction during test was larger in V1 than in any other visual area. MR signals were averaged from adapted regions (namely, the disk and annulus regions in the control-dynamic condition, the disk region in the jitter-annulus condition, and the annulus region in the jitter-disk condition) and MR signal intensity was summed during the first 10 s of the test period in each subject. A nonparametric test ($p < 0.01$, Friedman test) confirmed that the MR signal reduction was largest in V1 in each subject.

### Increased Signals in MT+

Thus far we have excluded MT+ from the analysis because the retinotopic analysis is not easily applicable to this cortical area (Tootell et al., 1998d). Now we will compare the nonretinotopic activities of visual areas including MT+ by summing up the voxels within each defined visual area. Figure 4 shows the time course of the MR signal change in each condition obtained by this nonretinotopic analysis. Thus except for area MT+, the data shown here are essentially an average of Figures 3A and 3B.

In both of the control conditions (where no jitter perception occurred), the MR signal did not increase during the test period (Figure 4, [3] and [4]). For example, MR signals in the control-static condition showed a flat time course. Likewise, in the control-dynamic condition, MR signals in retinotopic visual areas showed the expected decrease in the test period following the increase in the adaptation period: similar responses were previously observed in the retinotopic analysis. The behavior of MT+ was qualitatively similar to other areas in these conditions.

However, in both conditions jitter-disk and jitter-annulus (where jitter perception occurred in the disk and annulus regions, respectively), the MR signals in MT+ increased abruptly at the beginning of the test period (Figure 4, [1] and [2]). V3A (which is also motion selective [Tootell et al., 1997]), and V4v showed modest MR signal increases as well. Other cortical areas showed only minor positive-negative profiles, as expected from the data shown in Figure 3.

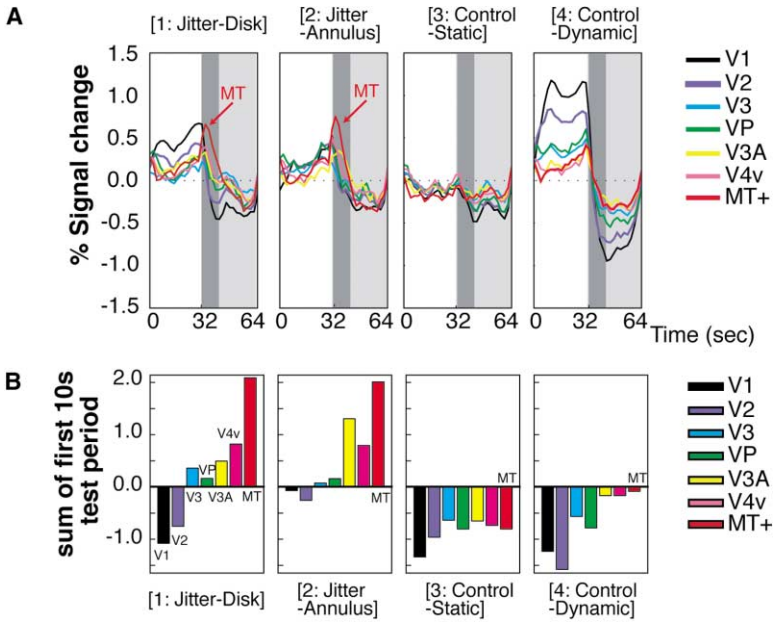


Figure 4. Time Course Results of the Nonretinotopic Analysis

(A) The latency-corrected time course of signal change in each visual area. MR signal changes in MT+ are colored red; otherwise the conventions are identical to those in Figure 3.

(B) MR signal integration over the first 10 s of the test period (dark gray in [A]).

Figure 4 shows that MT+ exhibited a prominent MR signal increase when visual jitter occurred. The MR signal increased very rapidly at the transition between the adaptation and test periods and rapidly decayed within roughly one-third of the test period. This time course is consistent with our perception of jitter: it appears most strongly at the beginning of the test period and typically lasts for 10–15 s (Murakami and Cavanagh, 1998, 2001).

Furthermore, a statistical test showed that the MR increase associated with jitter perception in the test period was larger in MT+ than in any other visual area. MR signals were averaged in conditions jitter-disk and jitter-annulus, and signal intensity was summed during the first 10 s of the test period in each subject. The signal increase in MT+ was significantly larger than in other visual areas (Friedman test, $p < 0.01$). Figure 4B shows this result more intuitively. The MR signal intensity was summed over the first 10 s of the test period for each visual area and plotted as a bar chart. The value of MT+ was greatest of all areas in conditions jitter-disk (Figure 4B, [1]) and jitter-annulus (Figure 4B, [2])—the two conditions in which illusory jitter was perceived.

To approximate our retinotopic analysis (e.g., Figure 2) in the less-retinotopic area MT+, we compared the levels of MT+ activation when jitter was confined within a single hemifield. Dynamic random noise was presented only in the left (or right) half of the visual field in the 32 s adaptation period, while static noise was presented in the opposite half of the visual field. In the subsequent 32 s test period, static noise was presented in both hemifields. In this configuration, jitter perception occurred in the right (or left) half of the visual field (i.e., in the unadapted region) when dynamic random noise ceased, as expected (Murakami and Cavanagh, 1998, 2001). Note that this approach is comparable to conditions jitter-disk and jitter-annulus in the main (retinotopic) analysis. To define a baseline activity level, we also included the control-static condition, in which static noise was presented in both hemifields in both periods (64 s in total). Again, we found that the MR signal in both the left and right MT+ showed increased MR signals during the test period when jitter perception occurred in either the left or the right half of the visual field.

## BOLD Undershoot

Following visual stimulation, the BOLD signals in area V1 show a transient decrease across many experiments and many stimuli. This so-called poststimulus undershoot (e.g., Kwong et al., 1992) is thought due to a temporal mismatch between the cessation of CBF (cerebral blood flow) increase, coupled with a slower recovery of CBV (cerebral blood volume) equilibrium associated with brain activity (Buxton et al., 1998; Hoge et al., 1999; Kruger et al., 1999; Mandeville et al., 1999a, 1999b, 1998). Here, we conducted a control experiment to see if the MR signal decrease after adaptation to dynamic random noise (see Figure 3) was simply another example of this poststimulus undershoot or whether an additional effect (as postulated here) was included.

The trial started with a blank period for 32 s. During such blank periods, the stimulus was a spatially uniform gray, of luminance equal to the mean luminance of the random noise; the central fixation point was always presented. In the subsequent 32 s period, the standard adapting stimulus was presented (as in the main experiment, e.g., Figure 1, [1] and [2]). In the following 64 s, subjects were presented with either of two conditions. In one condition (the jitter condition) we presented the same standard test stimulus used in the main experiment: static random noise in both the disk and annulus regions. Illusory jitter occurred in this stimulus. For the alternative undershoot condition, all visual noise was removed; thus the screen was spatially uniform except for the fixation point. Since the visual jitter illusion requires the presence of static noise, nothing appeared to move in this uniform screen. In this condition, the MR signal undershoot was expected to occur without the

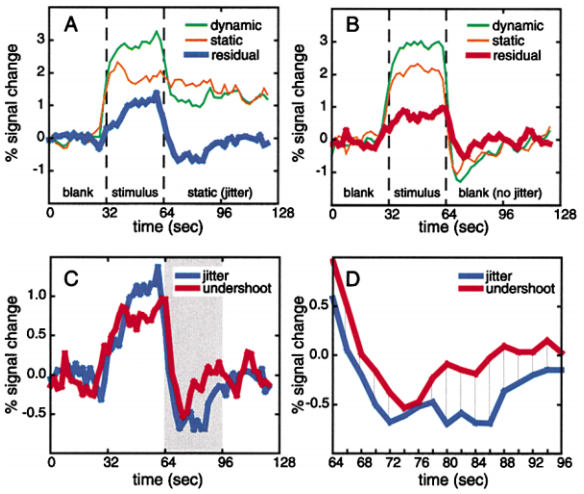


Figure 5. Results of Undershoot Control

(A and B) The time courses of MR signal decreases in V1 were averaged and plotted separately for the jitter (A) and undershoot (B) conditions. The signal change was defined relative to the baseline activity during the initial blank period. The green curve represents the averaged time course from the brain regions that were adapted to dynamic random noise, and the orange curve represents the averaged time course from the brain regions that were exposed to static random noise. The thick curves represent the residual brain activity between those two profiles.

(C) The overlay of the residual signals in the jitter and undershoot conditions is shown. The curves are colored consistently across panels. In the gray-coded interval, the MR signal reduction in the jitter condition remained low longer than the undershoot.

(D) Differences in the residual values in the third quarter are emphasized, with the time axis enlarged 400%; the ordinate is also enlarged slightly.

perception of illusory jitter. Our interest here was to see whether the signal decrease we had observed in the jitter condition was different from the signal decrease in the undershoot condition.

Figure 5 compares the time courses in the jitter condition (Figure 5A) and the undershoot condition (Figure 5B) in V1. In Figures 5A and 5B, the green and orange curves represent the time courses from the brain regions that were exposed to dynamic noise and static noise, respectively, during the adaptation period. The thick curve in each panel shows the difference (denoted as residual) between the green and orange. Thus, the blue curve in (A) corresponds to the effect of removal of flicker from the noise pattern, and the negative values during 64–96 s are considered to comprise the adaptational jitter effect. In (B), the green and orange curves showed the typical temporal profile of the BOLD undershoot, and the red curve in (B) corresponds to the residual difference between both undershoots. If the adaptational jitter effect was just another form of undershoot (with the background of static noise instead of the blank background) the residual signals in (A) and (B) would be equal because the background effect had been subtracted out. Figure 5C compares the residual curves from (A) (blue) and (B) (red). The residuals during the initial uniform period (0–30 s) and the last 32 s (96–126 s) were almost identical between the jitter and undershoot conditions, and they were nearly zero. Moreover, they were almost equivalent in the adaptation period (32–62 s).

Most importantly, the MR signal differed during the test period. This difference was most significant during the first half of the test period (64–94 s) when the jitter percept occurred. A nonparametric paired-comparison test revealed a statistically significant difference ($p < 0.0001$, two-tailed sign test) in this time period (64–94 s), as indicated by the shaded region (Figure 5C). Statistically significant differences were not found in any of the remaining time periods (e.g., 0–30 s, 32–62 s, etc.).

In Figure 5D, these third-quarter data are magnified. The difference reached near-significance even during the first 10 s (64–72 s) where most of the jitter perception occurs ($p = 0.0625$, two-tailed sign test), and the significance increased monotonically with longer sample times (for example, $p < 0.05$ for the first 12 s, $p < 0.002$ for the remaining 76–94s period). Thus, the MR signal reduction in the jitter condition was larger in amplitude, of longer duration, and was less erratic, compared to the undershoot condition. If the MR reduction in V1 (elicited by changing dynamic noise to static noise) was due to just the BOLD undershoot, the residual curve would be the same as in the undershoot condition. Therefore, even if there is a contribution from the undershoot effect to the MR signal reduction in V1, there is also a significant further decrease due to the adaptation.

## Discussion

Our fMRI experiments demonstrated that the BOLD activity of early cortical areas (e.g., V1) decreased after the corresponding retinotopic representation was adapted to dynamic random noise. Control tests confirmed that this decrease in V1 was distinguishable from the commonly described poststimulus undershoot, which is thought due to vascular phenomena. In contrast, in motion-selective/higher-tier cortical areas such as MT+ (and to a lesser extent V3A, and V4v), BOLD activity increased when illusory jitter perception occurred.

These results suggest a locus of adaptation in area V1 followed by a compensation mechanism for retinal slip located in the V1→MT+ pathway. This is consistent with the proposed model for visual jitter (Murakami and Cavanagh, 1998). This model proposed that a retinal-slip compensation mechanism explained the visual jitter illusion and also how retinal slip caused by small eye movements normally remains invisible. A unique and important point of this model is that it postulates two stages for this retinal slip correction mechanism: an adaptable motion measurement stage and a compensation stage (see Introduction). Consistent with this prediction, the MR signal decreased in early visual areas, such as V1, where dynamic random noise had been presented retinotopically (see Figures 2 and 3). This signal decrease may be interpreted to correspond to the adaptable motion measurement stage. In contrast, the MR signal was found to increase mainly in MT+ (and to some extent in V3A and V4v) when illusory jitter perception occurred, and this may correspond to the compensation stage.

Previous psychophysical experiments have revealed

that this jitter adaptation is monocular and selective for direction and spatial frequency (Murakami and Cavanagh, 1998, 2001). This suggests the involvement of early cortical areas such as V1. Consistent with this aspect of the model, we observed that the effect of adaptation on BOLD signals was most pronounced in V1 for our human subjects. The effect decreased progressively at higher-tier cortical levels.

On the other hand, two psychophysical facts suggest that the second (compensation) stage should occur at higher cortical levels. First, the jitter percept transfers between the left and right hemifields, even if the adapted and unadapted regions are separated up to 5°–6° (Murakami and Cavanagh, 2001). Second, jitter is greatest when the disk size matches the average receptive field size in the macaque MT at a given eccentricity (Murakami and Cavanagh, 2001). In agreement with these psychophysical findings, we have found that the BOLD signal in MT+ (which is bilaterally driven to some extent in humans [Tootell et al., 1998d, 1995b]) increased when jitter perception was present. The same pattern of MR signal increase was obtained both when adapted and unadapted regions were located concentrically and also when they were separated across the left and right hemifields. This is again consistent with size of the receptive field and bilaterality in primate MT/MST.

In fMRI studies, human MT+ is activated when a motion aftereffect is perceived in a physically stationary stimulus (Culham et al., 1999; He et al., 1998; Huk et al., 2001; Tootell et al., 1995a). Putting this fact together with the present finding, there is thus some superficial similarity in the MT+ responses to motion aftereffect and illusory visual jitter. In both cases, MT+ is active when one sees illusory motion in stationary stimuli. Additional evidence suggests that the activity of MT+ can be tightly related to one's perception of motion rather than actual motion information (Kourtzi and Kanwisher, 2000; Zeki et al., 1993).

Recently, Huk et al. (2001) pointed out that fMRI activation in human MT+ correlated with the perception of motion aftereffect can be confounded with the effect of attention. While attention could surely contribute to the present MR signal changes (e.g., in MT+), the following facts suggest that our effect is not entirely (nor even predominantly) due to attention. First, the BOLD signal showed both increases and decreases in different visual areas (e.g., MT+ and V1) simultaneously. Second, even within a visual area such as V1, the BOLD signal showed both an increase and decrease at the same time in retinotopic subdivisions consistent with the percept (e.g., Figure 2). Finally, in current experiments we have found the effect of attention modulates, but does not fully account, for conventional fMRI-based motion aftereffects (Sasaki, Y., Murakami, I., Watanabe, T., Tootell, R.B.H., and Nishida, N. (2002). Neuroimaging of direction-selective mechanisms for first-order and second-order motion stimuli. Paper presented at: Vis. Sci. Soc. Annual Meeting (Sarasota, FL).

After adaptation, why does V1 activity decrease and MT+ activity increase while we see jitter? Dynamic random noise has a flat spatiotemporal-frequency power spectra, containing a lot of motion energy in all directions at all speeds. This stimulus should strongly drive subcortical cells such as magnocellular LGN and V1 directionally selective cells as well, eventually desensitizing them. As a result, these cells should become less sensitive to incessant retinal slip during the test period. Such a transient loss of sensitivity should lead to decreased BOLD signals.

In contrast, according to the model (Murakami and Cavanagh, 2001), MT+ and some other extrastriate areas monitor the activity map of earlier stages such as V1 in order to calibrate the velocity field with respect to the minimum baseline. A biologically plausible way to do this would be to use center-surround antagonism with respect to motion, and in fact, such cells have been reported in areas MT and MST (Allman et al., 1985; Born et al., 2000; Born and Tootell, 1992; Tanaka et al., 1986). Such cells would fire when they detected objects moving faster than the background. Similarly, in jitter perception, they would also fire when they detected a faster motion velocity in a region (the unadapted region, in this case) compared to the transiently lowered baseline minimum in motion velocity in a region resulting from adaptation to dynamic random noise (i.e., the adapted region). Therefore, the positive BOLD signals in MT+ observed in this study are both theoretically feasible and consistent with the electrophysiological literature. Our current fMRI technique could not segregate MT from MST, but previous psychophysical measurements of the optimal stimulus size (Murakami and Cavanagh, 2001) suggest that MT may be more responsible for jitter perception than MST.

It has been asked why the V1 decrease is more sluggish (Figure 5D), compared to the apparently faster onset in the MT increase (Figure 4). First, this comparison is somewhat misleading because the V1 response is corrected for the undershoot, whereas the MT response is not. Secondly, differences as large as 0.25%–0.5% occur throughout the 64–96 s period (note that the blue curve is always lower than the red curve in Figure 5D), although those in the earlier half tend to be obscured by the steep decline of each curve. Third, it is certainly possible that the neural interaction between V1 and MT would not produce a simple linear MR inversion. Compared to the adapted population, many potential factors could reshape the MR signal in MT or V1, such as (1) threshold nonlinearities, (2) differences in the time course of gain control, and (3) fewer cells being involved in jitter perception. MR signals during visual illusion can have either a sharp onset (Tootell et al., 1995a) or a much slower onset (Hadjikhani et al., 1998)—even with equally abrupt onsets in percept. Hence, the minor difference in the shape of the time courses between V1 and MT remains compatible with our overall interpretation.

The BOLD signal increase associated with jitter perception also occurred to a lesser extent in visual areas such as V3A and V4v. Human V3A is known to be motion sensitive (Tootell et al., 1997) and thus may be directly involved in the perception of visual jitter. The degree of processing independence between cortical areas is unclear, but feedback signals may exist from human MT+ to V3A (Hupe et al., 1998). In the macaque, connections between MT and V3A have been reported, as well as between MT and V4 (Maunsell and Van Essen, 1983). V4v is one of the subdivisions of V4 (Boussaoud et al., 1991; Felleman and Van Essen, 1991; Gattass et al., 1988). Currently, how these cortical areas mutually inter-

act remains unsolved in humans (Tootell and Hadjikhani, 2001).

One of the fundamental tasks of visual processing from V1 to MT+ is considered to include visual motion processing. However, the present study suggests that these areas are also involved in stabilizing the visual world, processing visual motion inputs even during fixation of static scenes. V1, as the adaptation stage, registers retinal slip (although with lower gain after adaptation), providing inputs for subsequent compensation. MT+, as the compensation stage, uses these inputs and subtracts the minimum baseline motion from all other motions to counteract retinal slip. If these stages malfunction, then a static visual scene should not be perceived as static. That may be why some dyslexia patients who have reading difficulties and often complain that letters appear blurred and jittering (Stein and Walsh, 1997) reportedly show dysfunction in MT+ (Demb et al., 1997, 1998; Eden et al., 1996). In this respect, the underlying mechanisms of dyslexia patients' reading deficits and our illusory visual jitter may be similar to each other (G. Hebb, personal communication). This issue is currently open to investigation.

## Experimental Procedures

### Subjects

Eight healthy subjects with normal or corrected-to-normal visual acuity passively viewed visual stimuli in the magnetic resonance (MR) scanner. All subjects gave informed written consent. This study was approved by Massachusetts General Hospital Human Studies Protocol 96-7464 and 2000p-001155.

### Stimuli

Dynamic random noise was used as the adapting stimulus. 50% of the dots (each dot: 0.3° × 0.3°) were black (0.4 cd/m$^2$), and the remaining ones were white (62.7 cd/m$^2$); the background was gray (31.3 cd/m$^2$). The pattern was updated to a totally new pattern on each frame at 60 Hz. There were two concentric regions centered around the fixation point: a central disk (12° in diameter) and a surrounding annulus (30° in diameter) except for the interhemispheric tests, as described in the text.

### Conditions

A trial consisted of an adaptation period (32 s) and a subsequent test period (32 s) (Figure 1). In the adaptation period, each of the disk and annulus regions was filled with either dynamic random noise or static random noise. Hence, there were four varieties of adapting stimuli. In the jitter-disk condition, the annulus was dynamic and the disk was static. In the jitter-annulus condition, the annulus was static and the disk was dynamic. In the control-static condition, both annulus and disk regions were static. In the control-dynamic condition, both were dynamic. In the subsequent test period, the visual stimuli were always equivalent, namely, both disk and annulus regions were filled with static random noise. In the test period, jitter was perceived in the disk and annulus in conditions jitter-disk and jitter-annulus, respectively. In conditions control-static and control-dynamic, no illusory motion was perceived.

In each MRI scan (256 s), these four conditions (64 s each) were repeated in counterbalanced order across scans.

### Undershoot Control

We conducted another experiment to test the MR signal decrease observed after adaptation to dynamic noise, compared with an MR signal decrease expected from BOLD undershoot (Figure 5). We presented a blank screen with the fixation point (32 s) and then presented the same adapting stimulus (32 s) used in conditions jitter-disk (see Figure 1, [1]) or jitter-annulus (see Figure 1, [2]) in the main experiment. In the following test period (64 s), two possible stimuli were presented. In the jitter condition, the same static noise used in the main experiment was presented; in the alternative undershoot condition, a blank (spatially uniform gray) screen with the fixation point was presented instead of static random noise during this period.

For each condition, the time courses from the brain regions that were adapted to dynamic random noise were averaged across ROIs, hemispheres, and subjects. These data are plotted as green curves in Figures 5A and 5B (denoted as dynamic); these included the annulus region in the jitter-disk condition and the disk region in the jitter-annulus condition. Similarly, the time courses from the brain regions that were exposed to static random noise were averaged and plotted by orange curves (denoted as static).

### General Imaging Procedures

Experimental details were similar to those described elsewhere (Hadjikhani et al., 1998; Mendola et al., 1999; Somers et al., 1999; Tootell et al., 1997). Scans were acquired using either a 3T General Electric MR scanner retrofitted with ANMR echo-planar imaging or (in later experiments) a 3T Siemens Allegra. A custom-built, quadrature-based, semicylindrical surface coil was used to acquire high-sensitivity MR images including occipital, parietal, and posterior temporal lobes bilaterally. Voxels were 3.1 mm$^2$ in-plane and 3 mm thick. Functional MR images were acquired using gradient echo sequences (TE = 30 ms) with 128 images in 16 contiguous slices, oriented approximately orthogonal to the calcarine sulcus. TR was 2 s for the main fMRI experiments, and each fMRI scan took 256 s. Subjects were run for 8–15 scans for the purpose of signal averaging. A total of 75 functional scans (153,600 images) were obtained.

The statistical maps were generated using linear regression analysis. The fMRI signal was modeled as a linear convolution of a hemodynamic impulse function (Dale and Buckner, 1997). The activation amplitude for each condition was estimated from the fMRI time course on a voxel-by-voxel basis. T-tests were performed to compare activation amplitudes between conditions. Their p values were projected onto the flattened activity maps.

### Retinotopy

In a separate session, retinotopic visual areas and borders were mapped using phase-encoded stimuli and field sign analysis (Dale and Buckner, 1997; Hadjikhani et al., 1998; Sereno et al., 1995; Somers et al., 1999; Tootell et al., 1998a, 1997, 1998b, 1998c, 1998d). This analysis identified visual areas V1, V2, V3/VP, V3A, V4v, V7, and V8 (DeYoe et al., 1996, 1994; Engel et al., 1997; Schneider et al., 1993; Sereno et al., 1995; Tootell et al., 1998a, 1997, 1998b, 1998c, 1998d). Low-contrast, moving and stationary concentric rings were also presented to localize area MT+ (Beauchamp et al., 1997; Dupont et al., 1994; Lueck et al., 1989; McCarthy et al., 1995; Tootell et al., 1995a, 1995b; Watson et al., 1993; Zeki et al., 1991). Regions of interests (ROIs) were defined based on these functional borders. The TR was 4 s for retinotopic scans (8 min, 32 s duration) and 2 s for the MT+ localization (4 min, 16 s duration).

### Flattening the Visual Cortex

In a separate session, structural images of the whole brain were obtained with high resolution (1.0 × 1.0 × 1.3 mm$^3$, 1.5T) to provide data for three-dimensional reconstruction (Dale et al., 1999; Fischl et al., 1999), which allowed us to generate an unfolded and flattened cortical surface for each subject (FreeSurfer, http://www.nmr.mgh.harvard.edu/freesurfer).

## Acknowledgments

This study was supported by a grant from the National Eye Institute (EY07980) to R.B.H.T. Y.S. was supported by a fellowship from the Japan Society for the Promotion of Science. We thank Nouchine Hadjikhani for her technical assistance; Ken Kwong for his comments; Terrance Campbell, Larry Wald, Mary Foley, Larry White, and Bruce Rosen for MRI support; Tommy Vaughan for building the customized coil; and the Rowland Institute for machining MR-compatible hardware.

Received: August 10, 2001
Revised: June 17, 2002

## References

Allman, J., Miezin, F., and McGuinness, E. (1985). Direction- and velocity-specific responses from beyond the classical receptive field in the middle temporal visual area (MT). Perception *14*, 105–126.

Beauchamp, M.S., Cox, R.W., and DeYoe, E.A. (1997). Graded effects of spatial and featural attention on human area MT and associated motion processing areas. J. Neurophysiol. *78*, 516–520.

Born, R.T., and Tootell, R.B. (1992). Segregation of global and local motion processing in primate middle temporal visual area. Nature *357*, 497–499.

Born, R.T., Groh, J.M., Zhao, R., and Lukasewycz, S.J. (2000). Segregation of object and background motion in visual area MT: effects of microstimulation on eye movements. Neuron *26*, 725–734.

Boussaoud, D., Desimone, R., and Ungerleider, L.G. (1991). Visual topography of area TEO in the macaque. J. Comp. Neurol. *306*, 554–575.

Buxton, R.B., Wong, E.C., and Frank, L.R. (1998). Dynamics of blood flow and oxygenation changes during brain activation: the balloon model. Magn. Reson. Med. *39*, 855–864.

Culham, J.C., Dukelow, S.P., Vilis, T., Hassard, F.A., Gati, J.S., Menon, R.S., and Goodale, M.A. (1999). Recovery of fMRI activation in motion area MT following storage of the motion aftereffect. J. Neurophysiol. *81*, 388–393.

Dale, A., and Buckner, R. (1997). Selective averaging of rapidly presented individual trials using fMRI. Hum. Brain Mapp. *5*, 326–340.

Dale, A.M., Fischl, B., and Sereno, M.I. (1999). Cortical surface-based analysis. I. Segmentation and surface reconstruction. Neuroimage *9*, 179–194.

Demb, J.B., Boynton, G.M., and Heeger, D.J. (1997). Brain activity in visual cortex predicts individual differences in reading performance. Proc. Natl. Acad. Sci. USA *94*, 13363–13366.

Demb, J.B., Boynton, G.M., and Heeger, D.J. (1998). Functional magnetic resonance imaging of early visual pathways in dyslexia. J. Neurosci. *18*, 6939–6951.

DeYoe, E., Carman, G., Bandettini, P., Glickman, S., Wieser, J., Cox, R., Miller, D., and Neitz, J. (1996). Mapping striate and extrastriate visual areas in human cerebral cortex. Proc. Natl. Acad. Sci. USA *93*, 2382–2386.

DeYoe, E.A., Bandettini, P., Neitz, J., Miller, D., and Winans, P. (1994). Functional magnetic resonance imaging (FMRI) of the human brain. J. Neurosci. Methods *54*, 171–187.

Dupont, P., Orban, G.A., De Bruyn, B., Verbruggen, A., and Mortelmans, L. (1994). Many areas in the human brain respond to visual motion. J. Neurophysiol. *72*, 1420–1424.

Eden, G.F., VanMeter, J.W., Rumsey, J.M., Maisog, J.M., Woods, R.P., and Zeffiro, T.A. (1996). Abnormal processing of visual motion in dyslexia revealed by functional brain imaging. Nature *382*, 66–69.

Engel, S.A., Glover, G.H., and Wandell, B.A. (1997). Retinotopic organization in human visual cortex and the spatial precision of functional MRI. Cereb. Cortex *7*, 181–192.

Felleman, D.J., and Van Essen, D.C. (1991). Distributed hierarchical processing in the primate cerebral cortex. Cereb. Cortex *1*, 1–47.

Fischl, B., Sereno, M.I., and Dale, A.M. (1999). Cortical surface-based analysis. II: Inflation, flattening, and a surface-based coordinate system. Neuroimage *9*, 195–207.

Galletti, C., Squatrito, S., Battaglini, P.P., and Grazia Maioli, M. (1984). 'Real-motion' cells in the primary visual cortex of macaque monkeys. Brain Res. *301*, 95–110.

Gattass, R., Sousa, A.P., and Gross, C.G. (1988). Visuotopic organization and extent of V3 and V4 of the macaque. J. Neurosci. *8*, 1831–1845.

Gur, M., and Snodderly, D.M. (1987). Studying striate cortex neurons in behaving monkeys: benefits of image stabilization. Vision Res. *27*, 2081–2087.

Gur, M., and Snodderly, D.M. (1997). Visual receptive fields of neurons in primary visual cortex (V1) move in space with the eye movements of fixation. Vision Res. *37*, 257–265.

Gur, M., Beylin, A., and Snodderly, D.M. (1997). Response variability of neurons in primary visual cortex (V1) of alert monkeys. J. Neurosci. *17*, 2914–2920.

Hadjikhani, N., Liu, A.K., Dale, A.M., Cavanagh, P., and Tootell, R.B. (1998). Retinotopy and color sensitivity in human visual cortical area V8. Nat. Neurosci. *1*, 235–241.

He, S., Cohen, E.R., and Hu, X. (1998). Close correlation between activity in brain area MT/V5 and the perception of a visual motion aftereffect. Curr. Biol. *8*, 1215–1218.

Hoge, R.D., Atkinson, J., Gill, B., Crelier, G.R., Marrett, S., and Pike, G.B. (1999). Stimulus-dependent BOLD and perfusion dynamics in human V1. Neuroimage *9*, 573–585.

Huk, A.C., Ress, D., and Heeger, D.J. (2001). Neuronal basis of the motion aftereffect reconsidered. Neuron *32*, 161–172.

Hupe, J.M., James, A.C., Payne, B.R., Lomber, S.G., Girard, P., and Bullier, J. (1998). Cortical feedback improves discrimination between figure and background by V1, V2 and V3 neurons. Nature *394*, 784–787.

Ibbotson, M.R., and Maddess, T. (1994). The effects of adaptation to visual stimuli on the velocity of subsequent ocular following responses. Exp. Brain Res. *99*, 148–154.

Ilg, U.J., and Thier, P. (1996). Inability of rhesus monkey area V1 to discriminate between self-induced and externally induced retinal image slip. Eur. J. Neurosci. *8*, 1156–1166.

Kourtzi, Z., and Kanwisher, N. (2000). Activation in human MT/MST by static images with implied motion. J. Cogn. Neurosci. *12*, 48–55.

Kruger, G., Kastrup, A., Takahashi, A., and Glover, G.H. (1999). Simultaneous monitoring of dynamic changes in cerebral blood flow and oxygenation during sustained activation of the human visual cortex. Neuroreport *10*, 2939–2943.

Kwong, K.K., Belliveau, J.W., Chesler, D.A., Goldberg, I.E., Weisskoff, R.M., Poncelet, B.P., Kennedy, D.N., Hoppel, B.E., Cohen, M.S., Turner, R., et al. (1992). Dynamic magnetic resonance imaging of human brain activity during primary sensory stimulation. Proc. Natl. Acad. Sci. USA *89*, 5675–5679.

Leopold, D.A., and Logothetis, N.K. (1998). Microsaccades differentially modulate neural activity in the striate and extrastriate visual cortex. Exp. Brain Res. *123*, 341–345.

Lueck, C.J., Zeki, S., Friston, K.J., Deiber, M.P., Cope, P., Cunningham, V.J., Lammertsma, A.A., Kennard, C., and Frackowiak, R.S. (1989). The colour centre in the cerebral cortex of man. Nature *340*, 386–389.

Mandeville, J.B., Marota, J.J., Kosofsky, B.E., Keltner, J.R., Weissleder, R., Rosen, B.R., and Weisskoff, R.M. (1998). Dynamic functional imaging of relative cerebral blood volume during rat forepaw stimulation. Magn. Reson. Med. *39*, 615–624.

Mandeville, J.B., Marota, J.J., Ayata, C., Moskowitz, M.A., Weisskoff, R.M., and Rosen, B.R. (1999a). MRI measurement of the temporal evolution of relative CMRO(2) during rat forepaw stimulation. Magn. Reson. Med. *42*, 944–951.

Mandeville, J.B., Marota, J.J., Ayata, C., Zaharchuk, G., Moskowitz, M.A., Rosen, B.R., and Weisskoff, R.M. (1999b). Evidence of a cerebrovascular postarteriole windkessel with delayed compliance. J. Cereb. Blood Flow Metab. *19*, 679–689.

Maunsell, J.H., and van Essen, D.C. (1983). The connections of the middle temporal visual area (MT) and their relationship to a cortical hierarchy in the macaque monkey. J. Neurosci. *3*, 2563–2586.

McCarthy, G., Spicer, M., Adrignolo, A., Luby, M., Gore, J., and Allison, T. (1995). Brain activation associated with visual motion studied by functional magnetic resonance imaging in humans. Hum. Brain Mapp. *2*, 234–243.

Mendola, J.D., Dale, A.M., Fischl, B., Liu, A.K., and Tootell, R.B. (1999). The representation of illusory and real contours in human cortical visual areas revealed by functional magnetic resonance imaging. J. Neurosci. *19*, 8560–8572.

Murakami, I. (1995). Motion aftereffect after monocular adaptation to filled-in motion at the blind spot. Vision Res. *35*, 1041–1045.

Murakami, I., and Cavanagh, P. (1998). A jitter after-effect reveals motion-based stabilization of vision. Nature *395*, 798–801.

Murakami, I., and Cavanagh, P. (2001). Visual jitter: evidence for visual-motion-based compensation of retinal slip due to small eye movements. Vision Res. *41*, 173–186.

Schneider, W., Noll, D., and Cohen, J. (1993). Functional topographic mapping of the cortical ribbon in human vision with conventional MRI scanners. Nature *365*, 150–153.

Sereno, M.I., Dale, A.M., Reppas, J.B., Kwong, K.K., Belliveau, J.W., Brady, T.J., Rosen, B.R., and Tootell, R.B. (1995). Borders of multiple visual areas in humans revealed by functional magnetic resonance imaging. Science *268*, 889–893.

Somers, D.C., Dale, A.M., Seiffert, A.E., and Tootell, R.B. (1999). Functional MRI reveals spatially specific attentional modulation in human primary visual cortex. Proc. Natl. Acad. Sci. USA *96*, 1663–1668.

Stein, J., and Walsh, V. (1997). To see but not to read; the magnocellular theory of dyslexia. Trends Neurosci. *20*, 147–152.

Tanaka, K., Hikosaka, K., Saito, H., Yukie, M., Fukada, Y., and Iwai, E. (1986). Analysis of local and wide-field movements in the superior temporal visual areas of the macaque monkey. J. Neurosci. *6*, 134–144.

Tootell, R.B., and Hadjikhani, N. (2001). Where is 'dorsal v4' in human visual cortex? retinotopic, topographic and functional evidence. Cereb. Cortex *11*, 298–311.

Tootell, R.B., Reppas, J.B., Dale, A.M., Look, R.B., Sereno, M.I., Malach, R., Brady, T.J., and Rosen, B.R. (1995a). Visual motion aftereffect in human cortical area MT revealed by functional magnetic resonance imaging. Nature *375*, 139–141.

Tootell, R.B., Reppas, J.B., Kwong, K.K., Malach, R., Born, R.T., Brady, T.J., Rosen, B.R., and Belliveau, J.W. (1995b). Functional analysis of human MT and related visual cortical areas using magnetic resonance imaging. J. Neurosci. *15*, 3215–3230.

Tootell, R.B., Mendola, J., Hadjikhani, N., Ledden, P., Liu, A., Reppas, J., Sereno, M., and Dale, A. (1997). Functional analysis of V3A and related areas in human visual cortex. J. Neurosci. *17*, 7060–7078.

Tootell, R.B., Hadjikhani, N., Mendola, J., Marrett, S., and Dale, A. (1998a). From retinotopy to recognition: fMRI in human visual cortex. Trends Cogn. Sci. *2*, 174–183.

Tootell, R.B., Hadjikhani, N., Hall, E.K., Marrett, S., Vanduffel, W., Vaughan, J.T., and Dale, A.M. (1998b). The retinotopy of visual spatial attention. Neuron *21*, 1409–1422.

Tootell, R.B., Hadjikhani, N.K., Vanduffel, W., Liu, A.K., Mendola, J.D., Sereno, M.I., and Dale, A.M. (1998c). Functional analysis of primary visual cortex (V1) in humans. Proc. Natl. Acad. Sci. USA *95*, 811–817.

Tootell, R.B., Mendola, J.D., Hadjikhani, N.K., Liu, A.K., and Dale, A.M. (1998d). The representation of the ipsilateral visual field in human cerebral cortex. Proc. Natl. Acad. Sci. USA *95*, 818–824.

Wade, N.J., Swanston, M.T., and de Weert, C.M. (1993). On interocular transfer of motion aftereffects. Perception *22*, 1365–1380.

Watson, J.D., Myers, R., Frackowiak, R.S., Hajnal, J.V., Woods, R.P., Mazziotta, J.C., Shipp, S., and Zeki, S. (1993). Area V5 of the human brain: evidence from a combined study using positron emission tomography and magnetic resonance imaging. Cereb. Cortex *3*, 79–94.

Wohlgemuth, A. (1911). On the after-effect of seen movement. British Journal of Psychology Monograph Supplement *1*, 1–117.

Zeki, S., Watson, J.D., Lueck, C.J., Friston, K.J., Kennard, C., and Frackowiak, R.S. (1991). A direct demonstration of functional specialization in human visual cortex. J. Neurosci. *11*, 641–649.

Zeki, S., Watson, J.D., and Frackowiak, R.S. (1993). Going beyond the information given: the relation of illusory visual motion to brain activity. Proc. R. Soc. Lond. B Biol. Sci. *252*, 215–222.